Sensor and Simulation Notes

Note 371

Design Considerations for Ultra-Wideband, High-Voltage Baluns

Everett G. Farr
Farr Research

Gary D. Sower
EG&G, Inc.

C. Jerald Buchenauer
Phillips Laboratory

October 1994

Abstract

We consider here how to build a balun for fast-risetime pulses at high voltage. We are concerned with signals with risetimes on the order of 100-200 ps, with high peak voltages and peak powers. We propose the simplest method is a coaxial unzipper. We consider dielectric strength and maximum coaxial radius allowable while still maintaining the risetime. Also considered are methods to reduce the coupling to the common mode. Finally, we calculate the peak electric field and characteristic impedance of the coaxial unzipper at various point along its length using a two-dimensional Finite Element code.

I. Introduction

Many high-voltage impulse generators provide a high-voltage, fast-risetime pulse into a coaxial geometry. As the voltages increase and risetimes decrease, it will be necessary to develop the essential circuit components such systems require. A balun for such a system is a particularly challenging component to develop, due to competing demands for high dielectric strength of materials and small dimensions, in order to preserve the risetime.

We consider here the design principles required for baluns with voltages in the range of megavolts, powers in the range of tens of gigawatts to one hundred gigawatts, and risetimes in the range of 100-200 ps. We begin by providing a rationale for keeping the differential-mode impedance low, while keeping the common-mode impedance high. Next, we consider how to choose a feed impedance that keeps the electric field low for a given outer diameter of a cable. The dielectric properties of materials are then considered. We also provide a simple model for estimating the risetime that can be maintained through a given balun. Finally, we provide an example of numerical calculations, which would allow one to maintain a constant impedance through a coaxial unzipper, while keeping the peak field low.

Let us begin now with a simple explanation of why such a balun is necessary in the first place.

II. The Challenge of a Single-Ended Source

There are basically two challenges we may associate with a single-ended source. First, the field is arranged so that that it cannot be radiated efficiently. The radiated field on boresight for a transient antenna is proportional to the integral over the aperture distribution [1]. For a coaxial geometry, this integral is exactly zero, due to symmetry considerations (Figure 2.1). Thus, a different geometry is required, so a balun must be used.
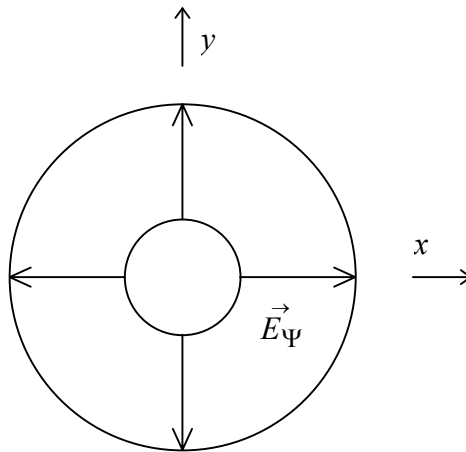

Figure 2.1. Electric fields in a coaxial geometry. Note that the integral over the aperture of E_y is zero by symmetry.

A second difficulty with a coaxial geometry involves the excitation of the common mode on the antenna, which decreases antenna efficiency. Consider the structure shown in Figure 2.2, which shows a coaxial cable that feeds a TEM horn. The exterior geometry consists of three conductors, the exterior of the cable and the two plates of the TEM horn. These three conductors can support two distinct modes, a differential mode and a common mode. The charges and electric fields associated with each of these modes is shown in Figure 2.3.

The differential mode is the mode that is desirable for radiation, since it sets up a potential difference between the plates of the TEM horn. The common mode is essentially lost energy, and it radiates in the wrong direction. Thus, we wish to minimize the energy in the common mode as much as possible. This is the second reason why baluns are necessary for this problem.
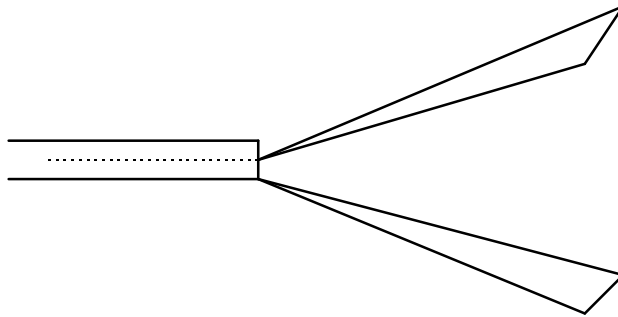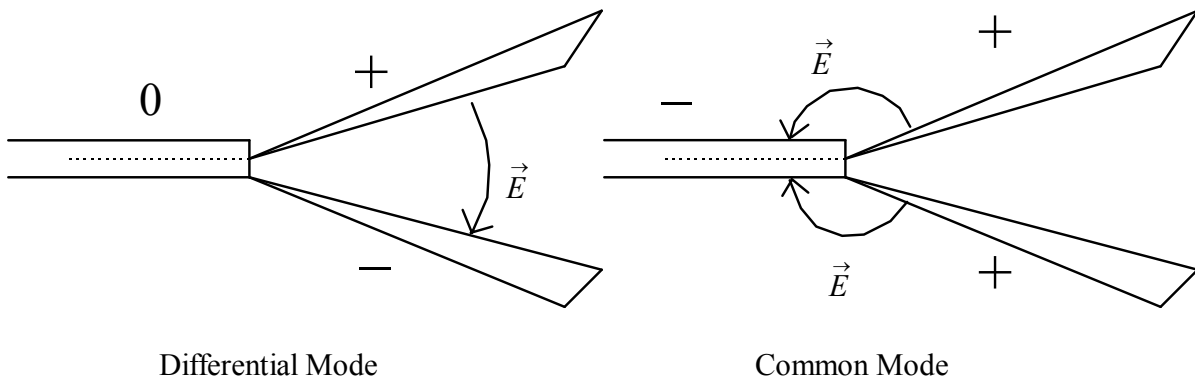
3

Figure 2.2. A TEM horn fed by a cable.

Differential Mode   Common Mode

Figure 2.3. A comparison of the charges and fields set up in differential mode and common mode.

III. The Importance of Keeping the Feed Impedance Low

Before building a balun, we must first give some thought to the impedance at which we build the balun. The output of this class of sources can be as low as 4–5 Ω. Antennas, on the other hand, tend to have an input impedance of 100-400 Ω. The impedance at which a balun is constructed can have a significant effect on the level of coupling to the common mode.

Let us consider now a highly oversimplified equivalent circuit for the configuration of Figure 2.2. The equivalent circuit is shown in Figure 3.1, and it assumes the coupling to the differential mode and common mode can be modeled by a simple resistance. (In fact, the impedance is a more complicated function of frequency, but we can still obtain useful information with a simple model.) To achieve the best efficiency, the impedance of the common mode should be large with respect to the impedance of the differential mode. Furthermore, the impedance of the differential mode should be matched to the feed cable.
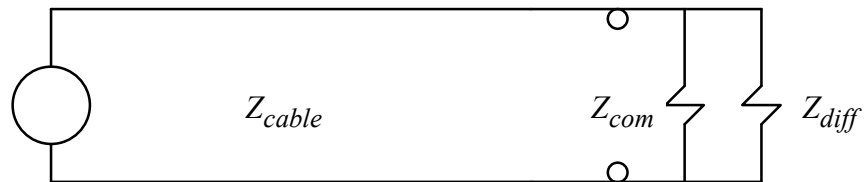

Figure 3.1. Equivalent circuit of the common and differential modes.

We can use this model to infer certain characteristics of a balun. First, it is advantageous to keep the differential-mode impedance low in the transition region. The impedance of the common mode is typically 200-300 Ω. Thus, one would like the differential mode impedance to be low compared to this. It is for this reason that we recommend trying to maintain the impedance somewhere below 50 Ω within the transition region. Note that this applies equally well to the unzipper balun shown in Figure 3.2.

The circuit model of Figure 3.1 also provides insight into the factors affecting the outer radius of an unzipper balun. One can increase the common-mode impedance by reducing the exterior diameter of the feed cable. Of course, when high voltages are involved this will have to be traded off against the dielectric strength of the material filling the cable. Note that a more detailed analysis of the coupling to the common mode could be obtained using the ideas in [2].

Ferrite

From Source $I_1 + I_2 \longrightarrow$ To Antenna

$I_2 \longleftarrow$

$I_1 \longrightarrow$

50 Ohm   Transition   50 Ohm   200 Ohm
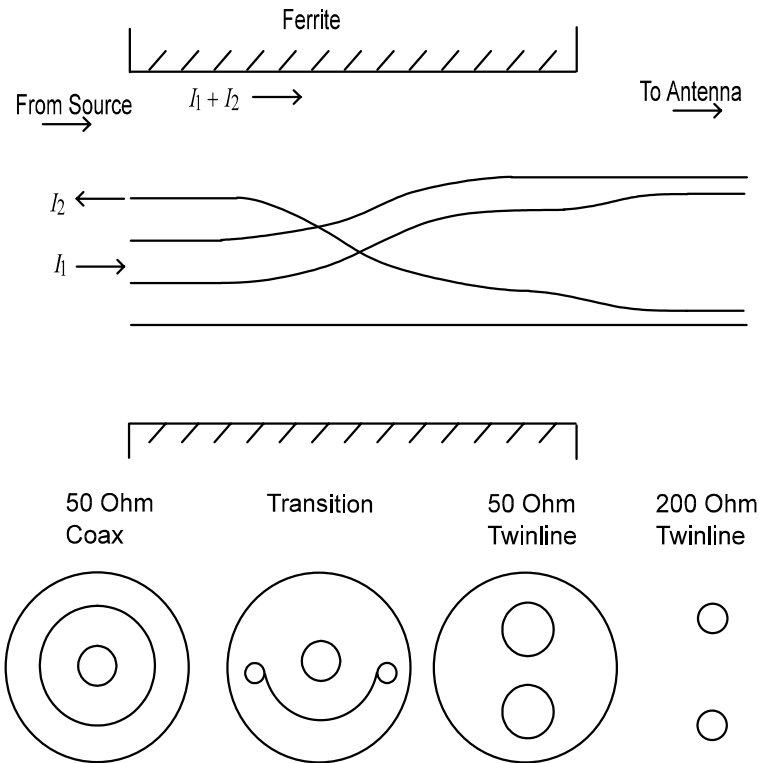Coax   Twinline   Twinline

Figure 3.2. The coaxial unzipper balun.

The model of Figure 3.1 also provides insight into where to locate the feed cable in a reflector IRA. One might consider, for example, feeding a reflector IRA by running a cable up through the center of the feed as shown on the left in Figure 3.3. However, with this arrangement the common mode impedance is quite low, since the cable is close to the conical arms. A better arrangement (with higher common-mode impedance) would be to have the cable approach the feed from behind, as shown on the right in Figure 3.3. A third arrangement, with the feed cable actually attached to one of the feed arms is also possible [3], and it might be better than the either of the two configurations shown in Figure 3.3, since no common mode could exist. But this would have a possible disadvantage of disturbing the conical geometry of the feed arms near the apex, where it is most critical.
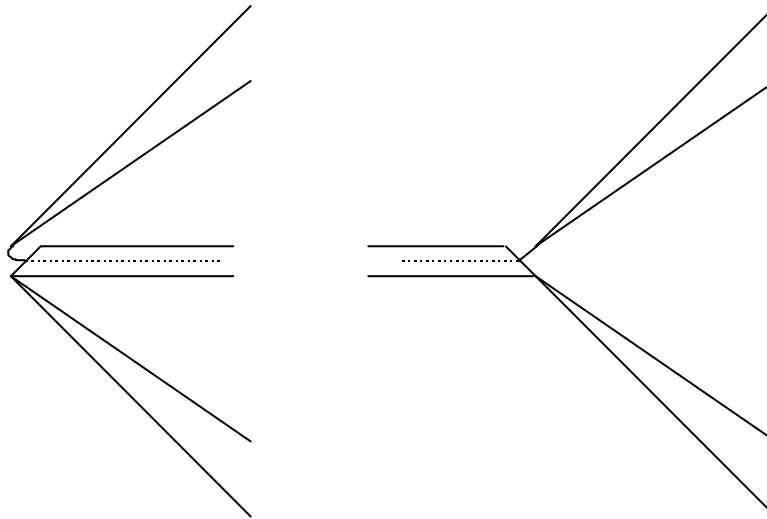
Figure 3.3. Possible feed arrangements for reflector IRA. The feed on the left is less desirable because its common-mode impedance is lower.

Thus, we have seen that we can reduce coupling to the common mode by keeping the impedance of the line low in the region of a transition. One gets the same effect by keeping the common-mode impedance large by using a small radius conductor. Note that one can also use ferrites or a ferrite/dielectric sandwich to increase the common-mode impedance, and this will be treated in another paper [4]. Nevertheless, it makes sense to reduce as much as possible the requirements on the ferrite, since the behavior of ferrites at fast risetimes and high field strengths remains somewhat new and unexplored.

IV. Optimization of Coaxial Cable Characteristics

We review here the electrical characteristics of coaxial cable. In doing so, we optimize the cable impedance in order to achieve maximum power transfer, for a given outer cable radius and maximum electric field. The configuration is shown in Figure 4.1.
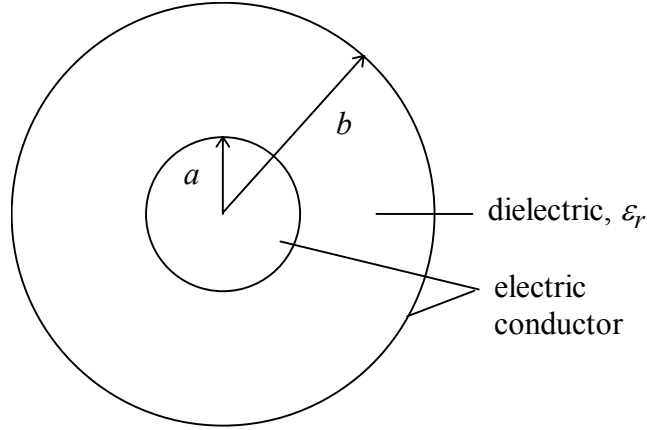

Figure 4.1. A coaxial geometry.

The characteristic impedance of a coaxial geometry is expressed as

$$Z_c = \frac{Z_o}{2\pi\sqrt{\varepsilon_r}}\ln(b/a)$$

$$f_g = \frac{Z_c}{Z_o}$$

(4.1)

where f_g is the geometric factor and $Z_o = \sqrt{\mu_o/\varepsilon_o}$ is the impedance of free space. The maximum electric field in the coaxial geometry occurs at the center of the geometry, and is equal to

$$E_{max} = \frac{V}{a\ln(b/a)} = \frac{V}{b}\frac{b/a}{\ln(b/a)}$$

(4.2)

From (4.1) we can express the ratio of the outer to inner radius in terms of the geometric factor as

$$\frac{b}{a} = e^{2\pi f_g\sqrt{\varepsilon_r}}$$

(4.3)

Substituting into (4.2), we find the maximum field as

8

$$E_{\text{max}} = \frac{e^{2\pi f_g \sqrt{\varepsilon_r}}}{2\pi f_g \sqrt{\varepsilon_r}} \frac{V}{b} \tag{4.4}$$

We find it convenient to express the above in terms of a normalized electric field, so

$$E_{\text{max}} = E^{norm} \frac{V}{b}$$

$$E^{norm} = \frac{e^{2\pi f_g \sqrt{\varepsilon_r}}}{2\pi f_g \sqrt{\varepsilon_r}} \tag{4.5}$$

This form makes it particularly convenient to find the maximum field in a coaxial geometry. We plot the normalized field as a function of impedance in Figure 4.2 for $\varepsilon_r = 1$ and for $\varepsilon_r = 2.2$.

We now wish to find the characteristic impedance that maximizes the peak power for a given peak electric field. The assumption here is that when a certain field level is reached, breakdown occurs. We therefore define a figure of merit that relates the peak electric field to the square root of the power on the line, for a given radius of the line. Thus, our figure of merit is

$$\eta = \frac{Z_o^{1/2} P^{1/2}}{b\, E_{\text{max}}} = \frac{V/f_g^{1/2}}{b(V/b)\, E^{norm}}$$

$$= \frac{1}{f_g^{1/2} E^{norm}} = \frac{2\pi f_g^{1/2} \sqrt{\varepsilon_r}}{e^{2\pi f_g \sqrt{\varepsilon_r}}} \tag{4.7}$$

The figure of merit η is unitless, and it is plotted in Figure 4.3 as a function of impedance. Note that the maxima in this figure of merit occur near $Z_c = 30\ \Omega$ for $\varepsilon_r = 1$ and $Z_c = 20\ \Omega$ for $\varepsilon_r = 1$. This suggests that a good choice for maximizing the peak power transferred through an unzipper type balun filled with SF_6 ($\varepsilon_r = 1$) would be about 30 Ω. Note, however, that the peak in this function is quite broad, so the exact impedance is not critical.
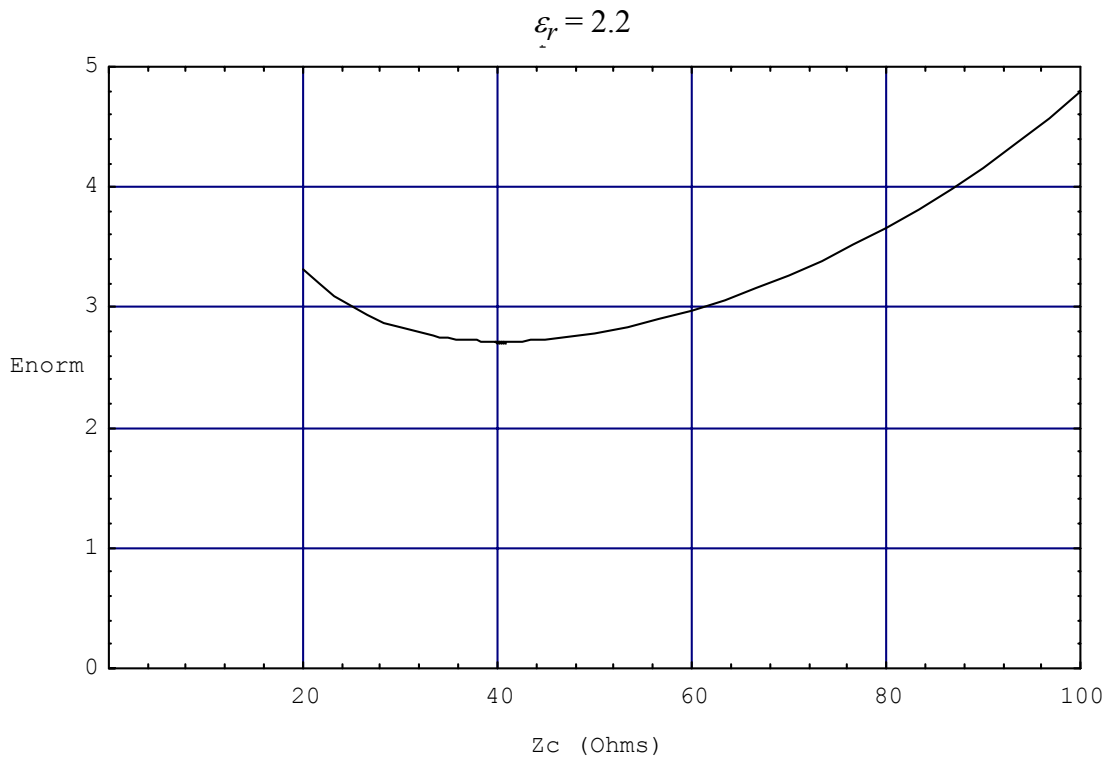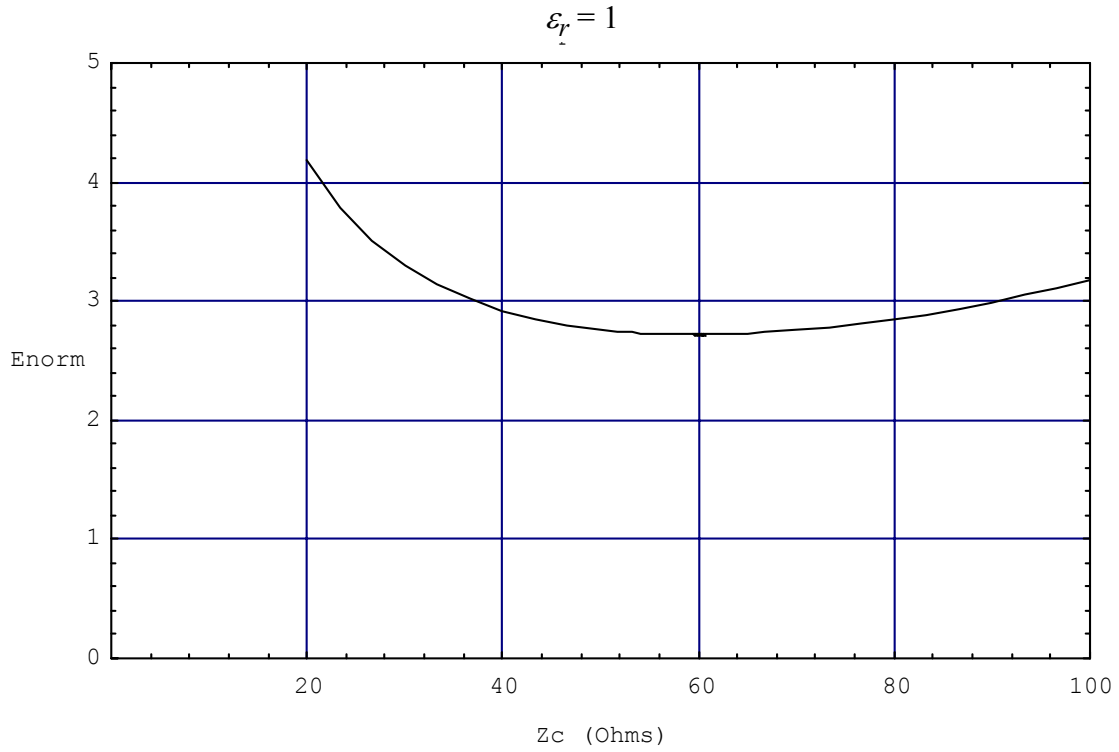
Figure 4.2 Normalized electric field as a function of impedance for $\varepsilon_r = 1$ (top) and for $\varepsilon_r = 2.2$ (bottom). Note the minima near $Z_c = 40$ Ω for $\varepsilon_r = 2.2$ and $Z_c = 60$ Ω for $\varepsilon_r = 1$.
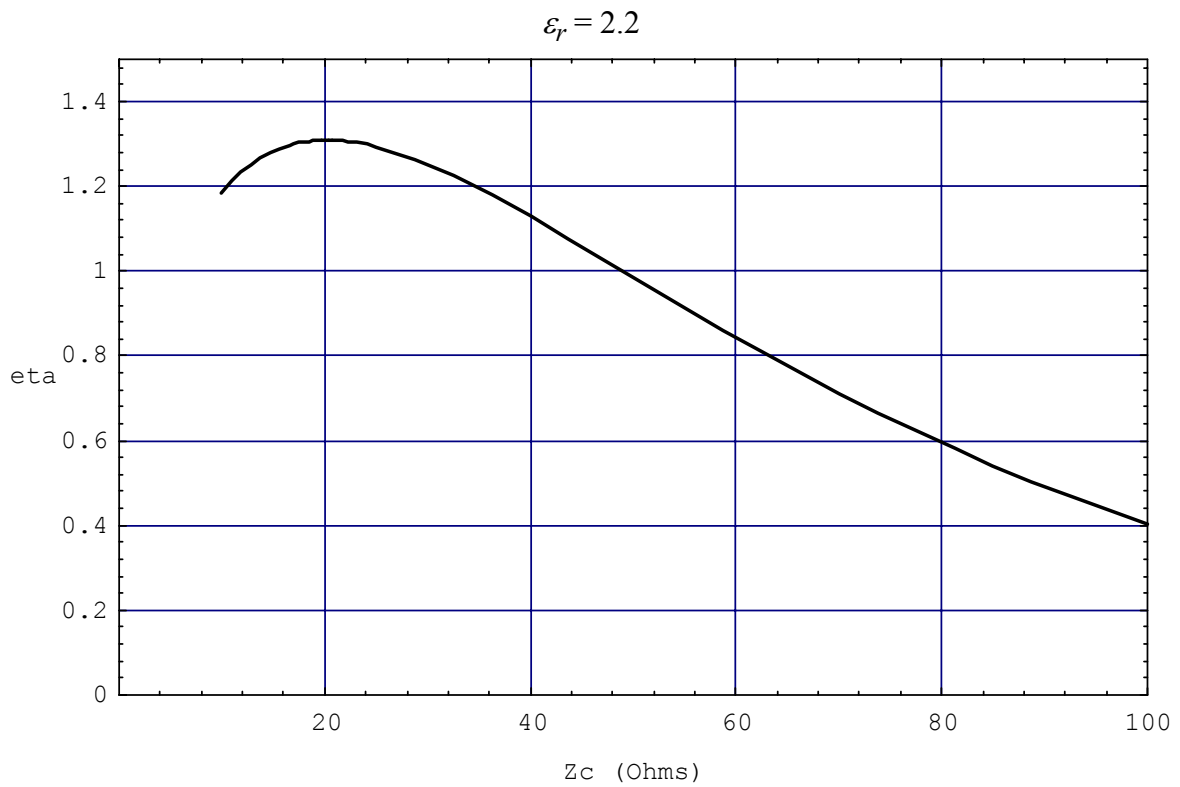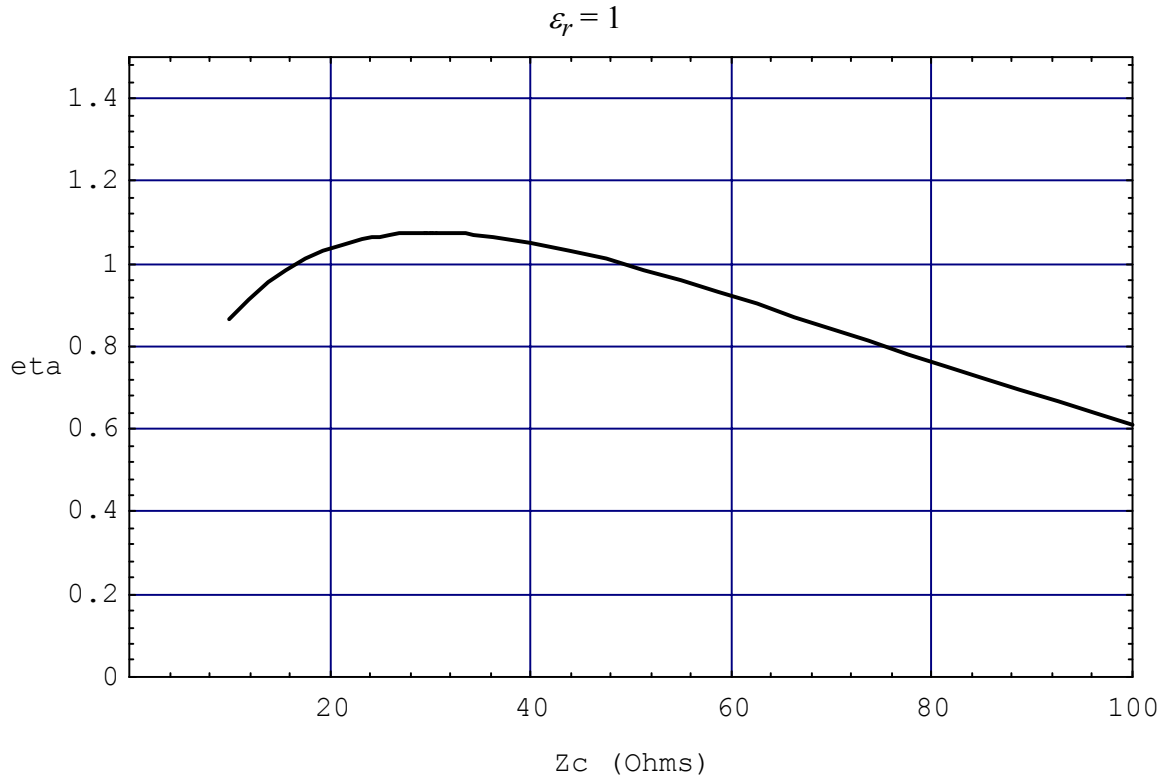
Figure 4.3. Efficiency factor for obtaining high power at low fields $\varepsilon_r = 1$ (top) and for $\varepsilon_r = 2.2$ (bottom). Note the maxima near $Z_c = 30\ \Omega$ for $\varepsilon_r = 1$ and $Z_c = 20\ \Omega$ for $\varepsilon_r = 1$.

V. Dielectric Strength of Materials

For many of the materials we might consider, there are simple laws for describing its dielectric strength. However, these laws are of limited utility for three reasons. First, these scaling laws were typically derived for longer pulse durations than those of interest here (300 ps – 1 ns). It is therefore unclear how well they will extrapolate to faster risetimes. Second, these laws are derived for single-shot operation, while we will often be interested in repetitive operation (perhaps as fast as 1 kHz). Finally, these scaling laws were derived for the purposes of a spark gap in a source, not for the large area of a transmission line. These considerations should be kept in mind as we describe the data available for various media.

A. Oil

The best data we have concerning breakdown of oil is provided by Larry Rinehart of Sandia National Laboratories [5]. He relates that the output section of SNIPER is a 50 Ω coaxial geometry in flowing oil with a one-inch outer diameter, and supports a 250 kV pulse lasting for 2 ns, with a repetition rate of 1 kHz. No breakdown is observed when the oil is flowing, however, if the oil is still, breakdown does occur. This corresponds to a peak field strength of 550 kV/cm. This suggests that we can support a 1 MV pulse with a 50 Ω cable of diameter 4 inches or 10 cm.

Note that the SNIPER pulse lasts for 2 ns, and in some cases one may be interested in a shorter . For faster pulse durations, one might scale the peak electric field sustainable as $t_{63}^{-1/3}$, where t63 is the pulse duration at 63% of the peak. We note, however, that there is no data yet available to confirm this scaling for such fast pulse durations, so it may be a bit optimistic to take full advantage of this scaling law. If we did take that effect into account, then a pulse of 300 ps length could be tolerated at a 1.9 times the field strength of a 2 ns pulse. In other words, if a cable could tolerate a 2 ps pulse at a voltage V_{max}, then it could tolerate a 300 ps pulse at a voltage of 1.9 V_{max}.

Another method of estimating the dielectric strength of oil is to use the standard formula for static breakdown of oil. We spoke with Ian Smith [6], who recommended using the standard formula, and then reducing the maximum field by a factor of four to allow for the 1 kHz repetition. The standard formula is [7]

$$E_{\max} \, t_{63}^{1/3} A^{0.075} \; < \; 0.48 \tag{5.1}$$

where E_{max} is the maximum electric field in MV/cm, t_{63} is the duration of the pulse in μs at 63% of the maximum, and A is the area in cm^2 of the center conductor. The above rule applies to the worst-case where the center conductor is positive. If the center conductor has negative polarity, the field can be higher by a factor of $2^{1/2}$, or 1.4. The area of the center conductor is just

$$A = 2\pi a \ell \tag{5.2}$$

where ℓ is the length of the transition, and a is the radius of the center conductor.

As an example, let us assume we are designing for a 50 Ω cable with an outer diameter of $b = 5$ cm and a length of $\ell = 100$ cm. Recall that for a 50 Ω coax line in oil, $b/a = 3.44$, so we have $a = 1.46$ cm, and $A \approx 791$ cm^2. We also assume the pulse lasts for 0.3 ns, or 0.0003 μs. Using (1), we find we must keep $E_{max} < 4.35$ MV/cm in order to avoid breakdown in single-shot mode. Using Smith's rule of allowing only one-fourth the normal breakdown field for repetitive mode, we can support 1.1 MV/cm. This result is similar to that obtained by extrapolating Larry Rinehart's data (above). so it seems reasonable.

B. Polyethylene

Since standard cables are often built with polyethylene, this material is also of interest. Again, some of the best available data comes from verbal discussions with Larry Rinehart concerning tests on an RG-220 line. This line was pulsed for 1.3 million shots at 10 Hz with a 300 kV pulse of duration 460 ns FWHM. Note that RG-220 cable has a one-inch outer diameter, and is filled with polyethylene. This generates a peak electric field on the center conductor of about 660 kV/cm. This is comparable to the dielectric strength of flowing oil, as calculated above.

Note that the testing at Sandia reported by Rinehart never went as far as actual breakdown, since they were using the largest source they had. Thus, polyethylene may actually have a somewhat higher dielectric strength than these numbers indicate. Difficulties were reported, however, at the connectors, so that may be where the real difficulty lies.

Note also that polyethylene has the property that it can deteriorate over time. Thus, one can operate in a region below breakdown field strengths, and still have a part fail after many shots.

C. Sulfur Hexafluoride

The standard formula for gas breakdown is [8]

$$\rho\tau \ = \ 97800\,(E\,/\,\rho)^{-3.44} \tag{5.3}$$

where ρ is the gas density in gm/cc, τ is the time delay to breakdown in seconds, and E is the average electric field in kV/cm. This can be rearranged into another form as

$$E \ = \ (97800\,/\,\tau)^{0.291}\,\rho^{0.709} \tag{5.4}$$

The gas density of some common gasses is are shown in Table 5.1. This values have to be multiplied by the pressure of the gas (in atmospheres), to get the total gas density at high pressure.

Table 5.1. Density of some common gases

Gas	Density at 1 atmosphere (g/cc)
SF_6	6.5×10^{-3}
H_2	0.089×10^{-3}
N_2	1.25×10^{-3}

As an example, consider the dielectric strength of SF_6 at 20 atm., which is about as high a pressure as one can have before the gas condenses. For a pulse of 300 ps duration, we find we can withstand an average electric field of 4 MV/cm. This is actually somewhat higher than what we have calculated for oil or polyethylene. However, for those cases, we attempted to consider the effect of a fast repetition rate. In this case we have no adjustments available for rep rate.

We spoke recently with Tom Martin [10] concerning SF_6 breakdown, and effects due to repetition rate. He suggested that a mixture of sulfur hexafluoride (20%) and air could have eighty percent of the dielectric strength of pure SF_6, at lower cost. Furthermore, if one has to worry about recovery times of the gas associated with repetition rates, the 20% mixture has a much faster recovery time, and may be more suitable for a repetitive environment.

VI. Bandwidth/Risetime Considerations

While dielectric breakdown considerations push the design in the direction of large components, bandwidth/risetime considerations push the design in the direction of having small components. This is especially true of a design that must preserve a risetime in the range of 100–200 ps. Thus, we require some estimate of the risetime that can be preserved in a balun such as that shown in Figure 3.2. We consider two methods of calculating this effect. First, we provide an approximate model derived from first principles. Second, we compare our configuration to a similar piece of hardware that has already been built and tested.

A. Simple theory of risetimes

We now consider a simple model for the risetime of an unzipper balun, by comparing the lengths of the shortest and longest ray paths. This technique is similar to one used earlier by Baum [11]. Consider the lengths of the shortest and longest ray paths through the balun. The shortest ray path is just the length of the unzipper, ℓ. The longest ray path is approximately the length added in quadrature to half of the outer circumference (Figure 6.1), or

$$
\begin{aligned}
\ell_{long} &= \sqrt{\ell^2 + (\pi b)^2} \\
&\cong \ell\left[1 + \tfrac{1}{2}(\pi b / \ell)^2\right] \qquad b << \ell
\end{aligned}
\tag{6.1}
$$

The difference in ray path lengths is just

$$
\begin{aligned}
\ell_{extra} &= \ell_{long} - \ell \\
&\cong \frac{\pi^2 b^2}{2\ell}
\end{aligned}
\tag{6.2}
$$

This distance then has to be converted to units of time for a particular dielectric. Thus the delay time is

$$
t_{delay} = \frac{\sqrt{\varepsilon_r}\ \ell_{extra}}{c} \cong \frac{\sqrt{\varepsilon_r}\ \pi^2 b^2}{2\,\ell\,c}
\tag{6.3}
$$

Finally, we must determine the relationship between the delay time and the risetime the structure can support. We estimate that a balun can tolerate a delay time equal to the risetime of the output pulse. The pulse will then be centered at one-half the delay time, and no ray will differ from the average by more than half the risetime. Thus, we have the rule

16

$$t_r = K \frac{\sqrt{\varepsilon_r}\, b^2}{\ell\, c}$$

$$K = \frac{\pi^2}{2} = 4.9$$

(6.4)

where t_r is the risetime of the pulse. Note that there has previously been some speculation that the time delay through a balun is proportional to D^2/ℓ, where D is the diameter. The rule we have derived is consistent with that rule, and it shows why the rule is reasonable.

As an example, let us assume we must maintain a pulse of 150 ps risetime through a radius of 9 cm in SF_6 with $\varepsilon_r = 1$. This would indicate a length of 88 cm is required to maintain the risetime.

Input Cross Section
$z = 0$

Output Cross Section
$z = \ell$

$2b$

Path of Longest Ray
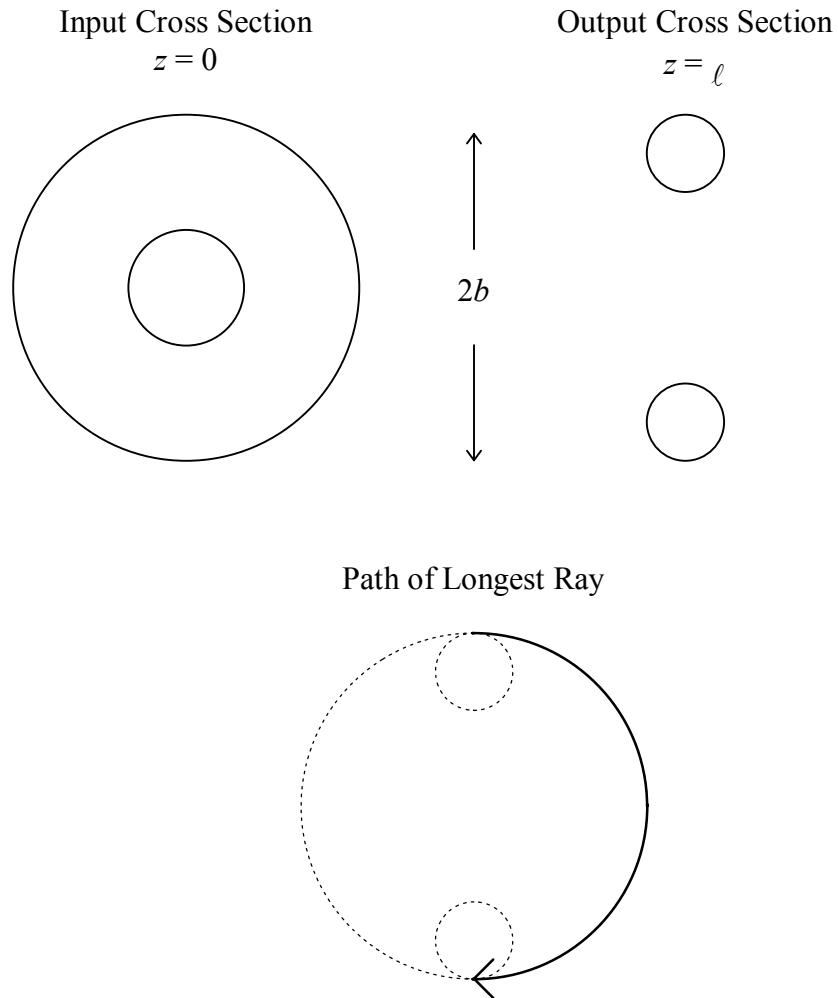
Figure 6.1. Geometry for tracing the longest path through a balun.

B. The ARES Transition

To test this hypothesis, and in particular, to check the proportionality constant K from the previous section, we consider data available from the ARES EMP test facility, in Albuquerque. At ARES there is a coaxial unzipper in SF_6, where they wish to preserve a 1 ns risetime, through a coaxial unzipper whose diameter is 122 cm (Figures 6.1 and 6.2) [12]. The transition length is 228 cm. Substituting all the above information into (6.4), we find a value of K=1.8. This suggests that equation (6.4) is conservative by a factor of 2.7. In other words, the ARES transition has a length that is 2.7 times shorter than equation (6.4) requires, and still maintains the required risetime.

A reasonable approach to resolving the discrepancy would be to build a number of baluns of this type, and measure the fastest risetime that can be sustained. In future work we will try to do this.
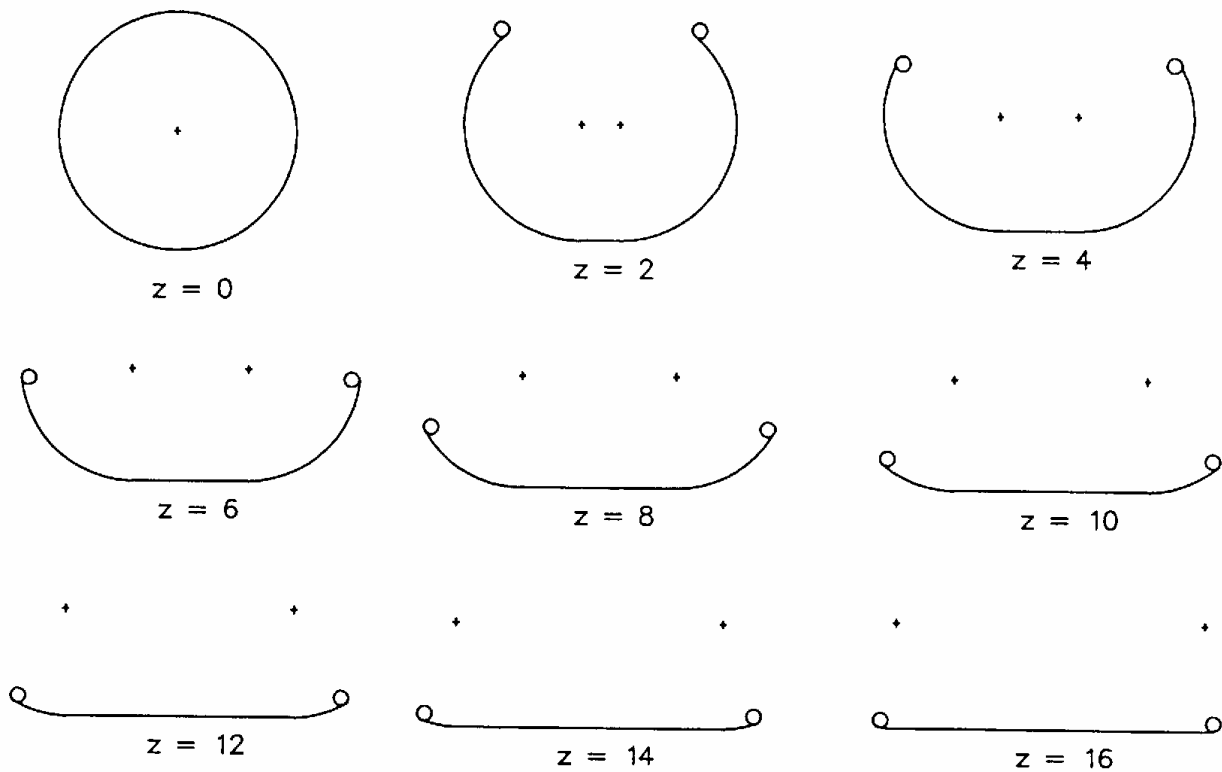

Figure 6.1. Unfolding of the ARES transition. Dimensions are in inches for a one-fifth scale model of the actual transition as built at ARES.
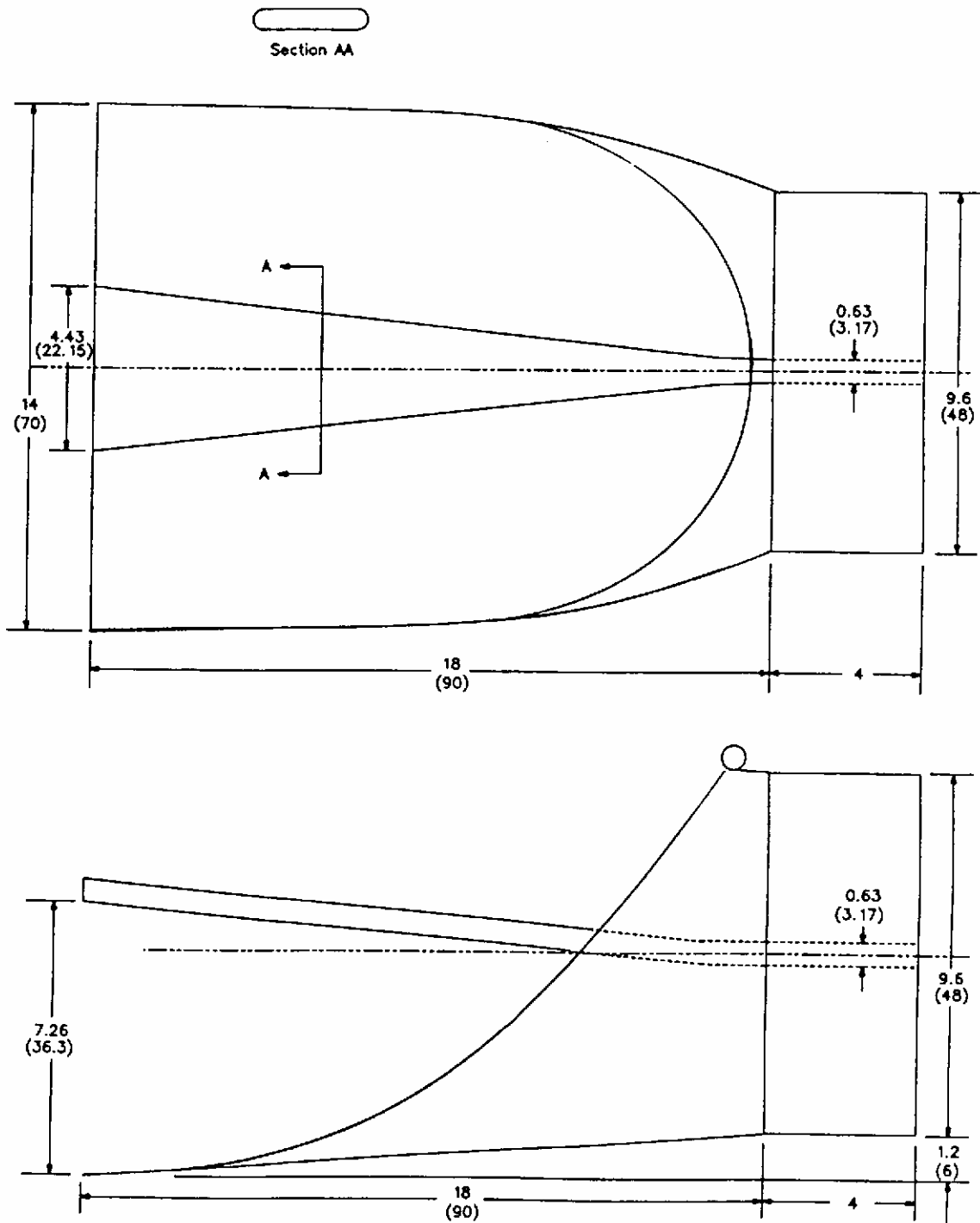
Figure 6.2. Transition section at ARES. Dimensions in parentheses are for the full-scale device as installed at ARES, in inches. Dimensions not in parentheses are for a one-fifth scale model, also in inches.

VII. Numerical Calculations of the Cross Section

We consider here the solution of a problem we consider to be typical. We wish to maintain a 50 Ω impedance through an oil-filled unzipper section with a radius of 5 cm. Note that based on the results of section IV, one might wish to use a somewhat lower impedance for an oil-filled line, if optimal power transfer is required.

The analysis is performed using a 2D finite element program called *Maxwell*, from Ansoft Corporation. This provides an adaptive 2D solution to Laplace's equation with boundary conditions suitable for infinite boundaries. It also provides a check of the error in a given triangle, and will further subdivide a region where an error specification is not met. Thus, one ends up with a higher density of triangles in regions where the field changes most rapidly.

We began by estimating the 2D cross sections that could support the wave at various points along the unzipper. After adjusting the geometries to a 50 Ω impedance, we arrived at the five geometries shown in Figure 7.1. In addition to the characteristic impedance, Maxwell can calculate the magnitude of the electric field, and the electric potential, and these are shown in Figures 7.2 and 7.3. These plots required somewhere between 230 and 500 triangles to achieve an energy error of <0.1% and a residual of 10^{-6}. The conclusion one can draw from the graphs is that one can indeed open up a coaxial line without enhancing the field beyond what is seen in the original coax.

One can estimate the accuracy of the technique by comparing the results for the coaxial geometry to theory. For this geometry we expect to calculate 50 Ω and a peak electric field of 550 kV/cm. We have calculated an impedance of 49.89 Ω and a peak field of 559 kV/cm, for an error of 0.3 % and 3.5%, respectively. Note that the impedance is more accurate than the peak field, but this should be sufficient accuracy for our purposes.

One can conclude from these calculations that the highest electric field in oil occurs in the coaxial cable. At points further along in the unzipper structure the peak field decreases somewhat. It may be useful later to provide a similar analysis for $\varepsilon_r = 1$, i.e., for air or SF_6. Nevertheless, we expect the same trend to hold.

Figure 7.1. Drawings of the cross sections. (Dimensions are in centimeters.)
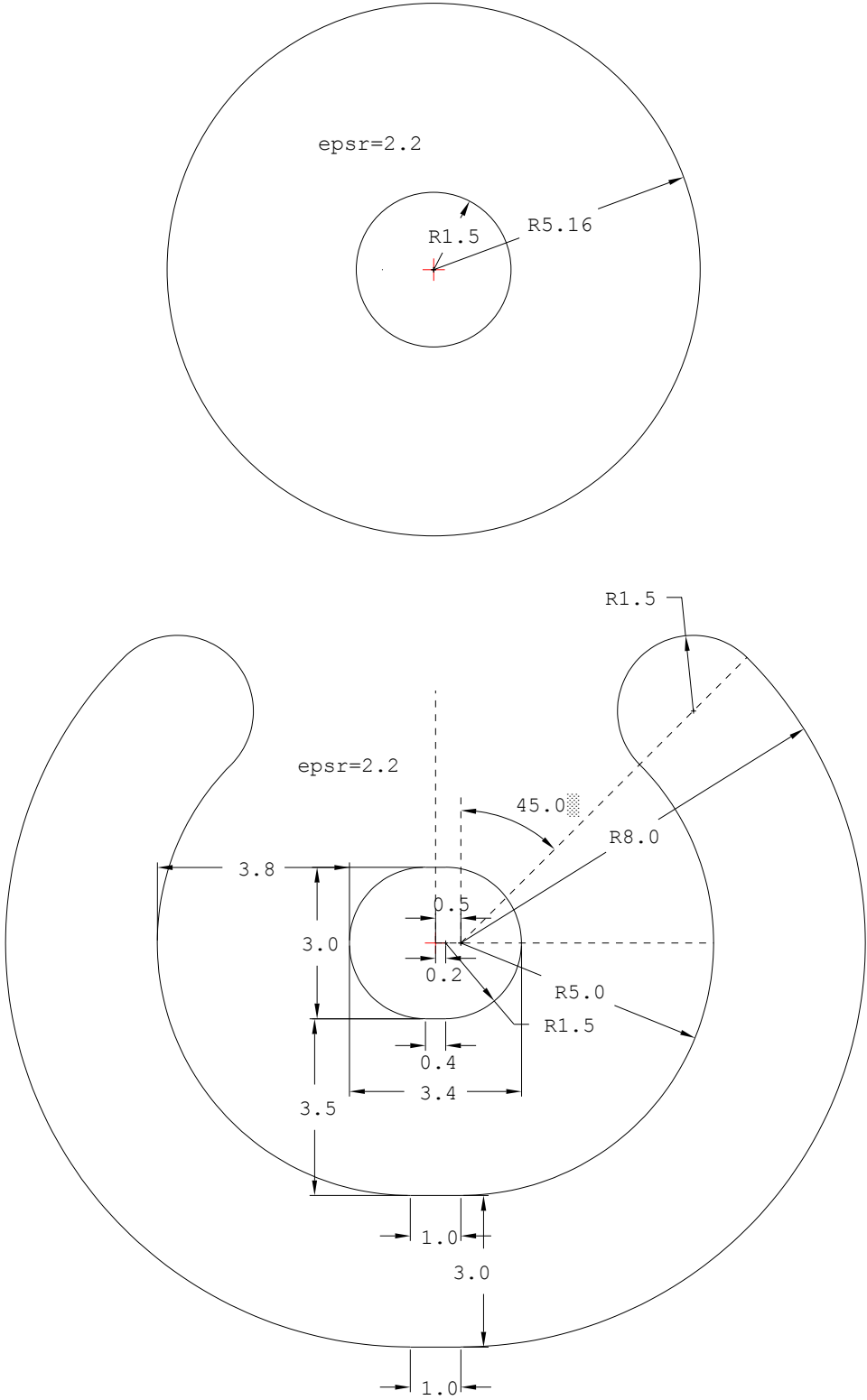
epsr=2.2

R1.5

R5.16

R1.5

epsr=2.2

45.0

R8.0

3.8

3.0

0.5

0.2

R5.0

R1.5

0.4

3.4

3.5

1.0

3.0

1.0

Figure 7.1. (con'd)

epsr=2.2

3.65

3.0

.85
1.0

1.7

4.7

3.5

R1.5

90.0

R1.5

R5.0

R8.0

R1.5

2.0

3.0

2.0

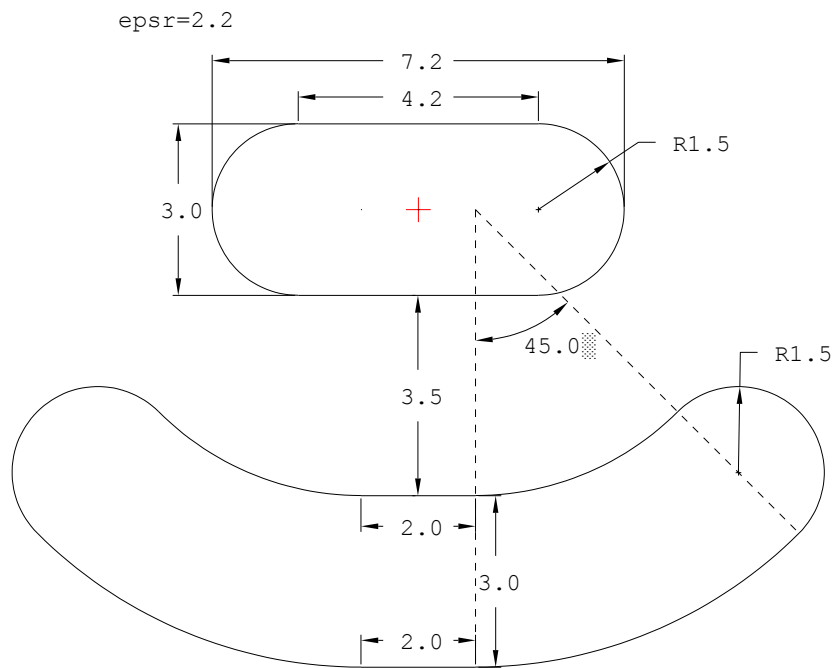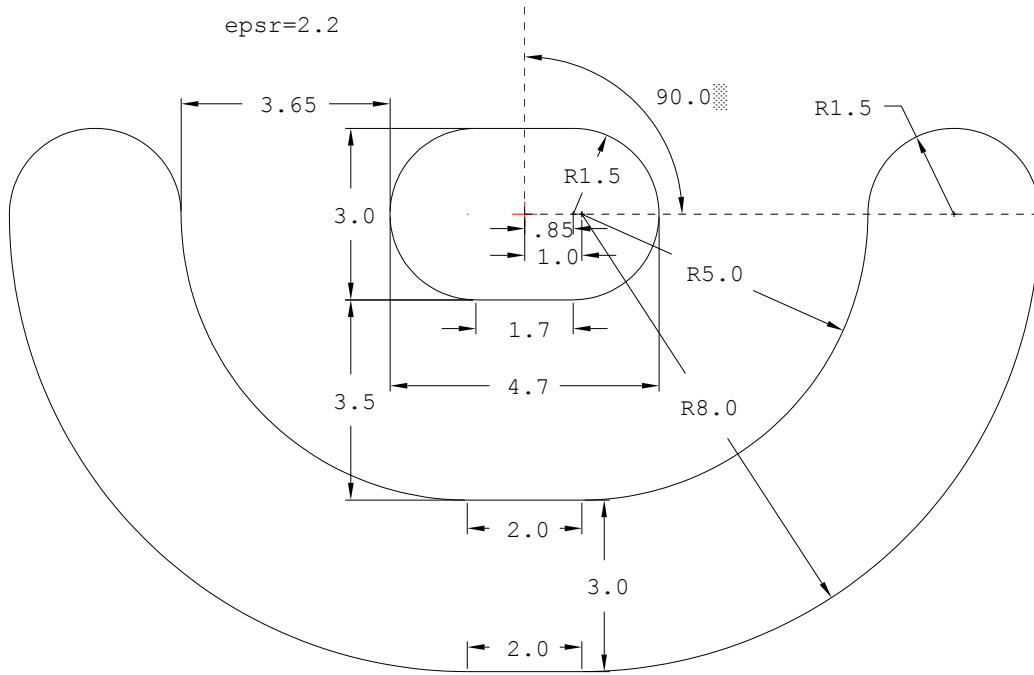epsr=2.2

7.2

4.2

3.0

R1.5

45.0

R1.5

3.5

2.0

3.0

2.0

22

Figure 7.1. (con'd)
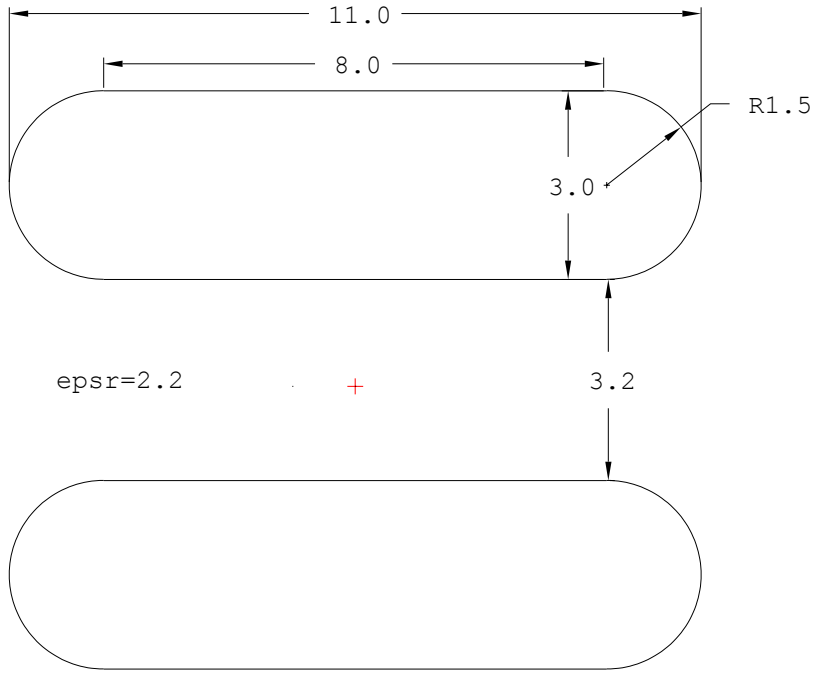
Figure 7.2. Magnitude of the electric field calculated by Maxwell. (Scale is in V/m.)

Mag E

5.5853e+007
5.1776e+007
4.7700e+007
4.3623e+007
3.9547e+007
3.5470e+007
3.1394e+007
2.7317e+007
2.3241e+007
1.9164e+007
1.5088e+007

Figure 7.2. (con'd)

Mag E

5.3850e+007
4.8465e+007
4.3080e+007
3.7695e+007
3.2310e+007
2.6925e+007
2.1540e+007
1.6155e+007
1.0770e+007
5.3850e+006
1.0659e+000
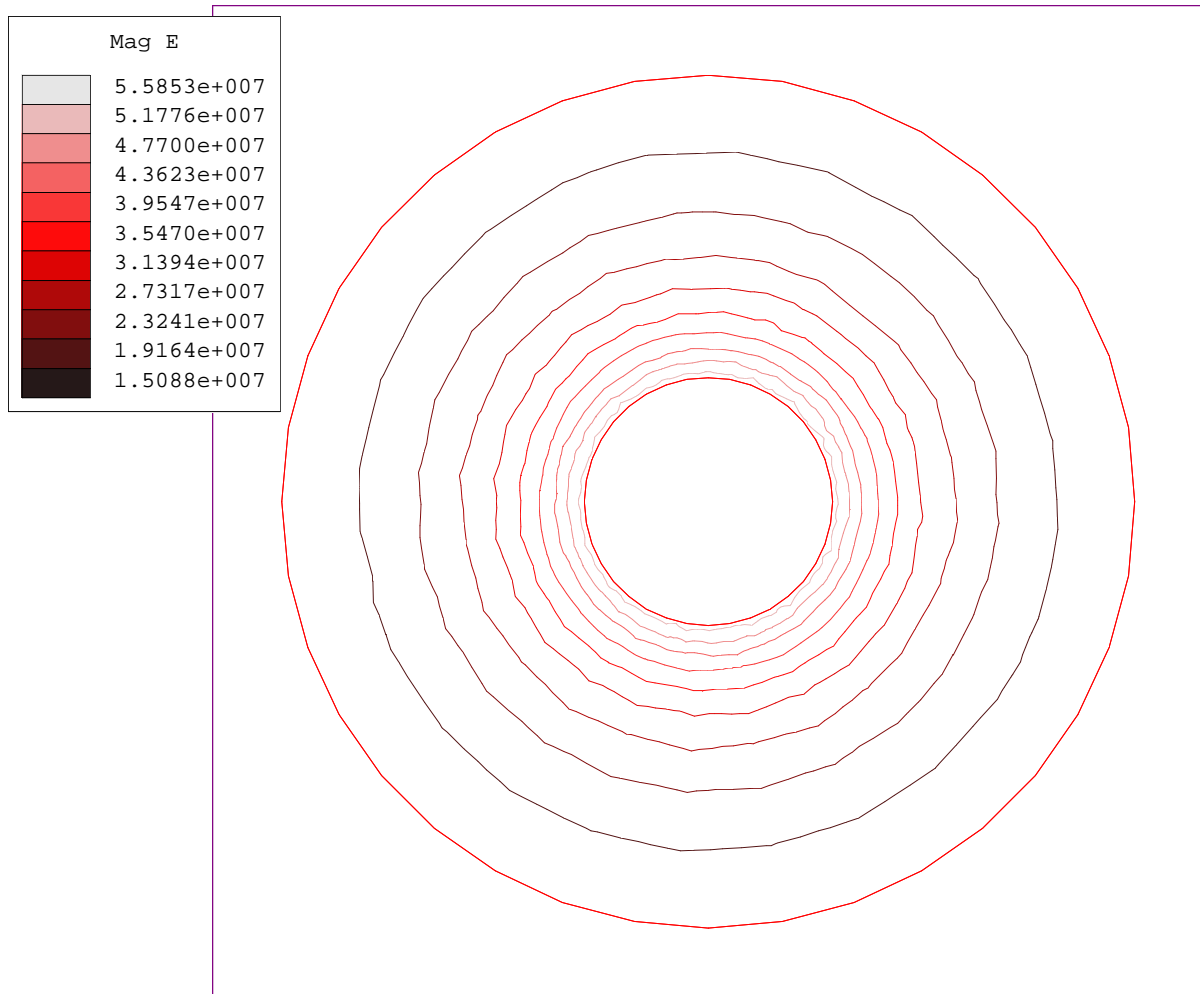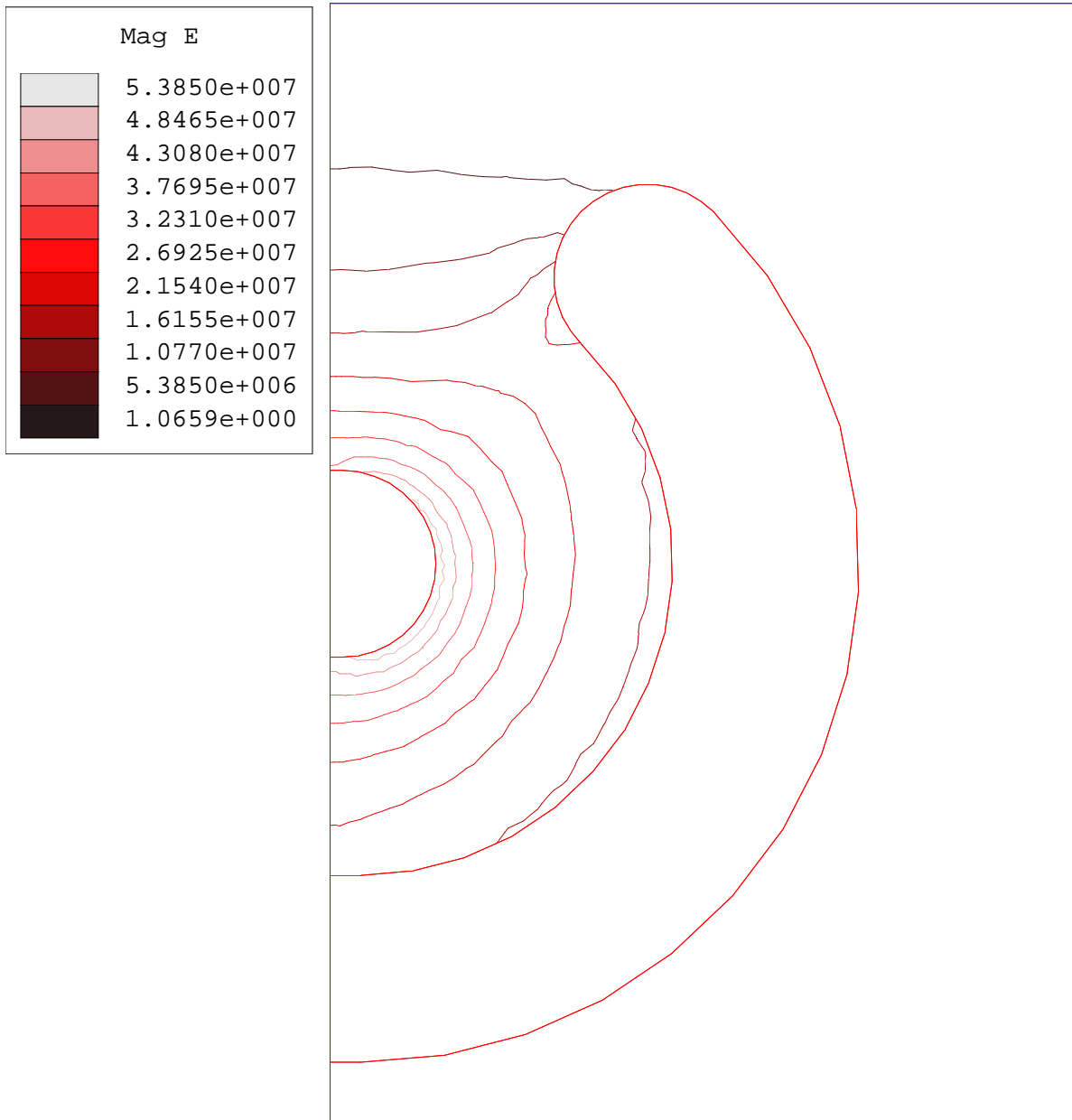
Figure 7.2. (con'd)

Figure 7.2. (con'd)

Mag E

	5.3271e+007
	4.7944e+007
	4.2617e+007
	3.7290e+007
	3.1963e+007
	2.6636e+007
	2.1308e+007
	1.5981e+007
	1.0654e+007
	5.3271e+006
	4.1639e+000

Figure 7.2. (con'd)

Mag E

3.8276e+007
3.4449e+007
3.0621e+007
2.6793e+007
2.2966e+007
1.9138e+007
1.5310e+007
1.1483e+007
7.6552e+006
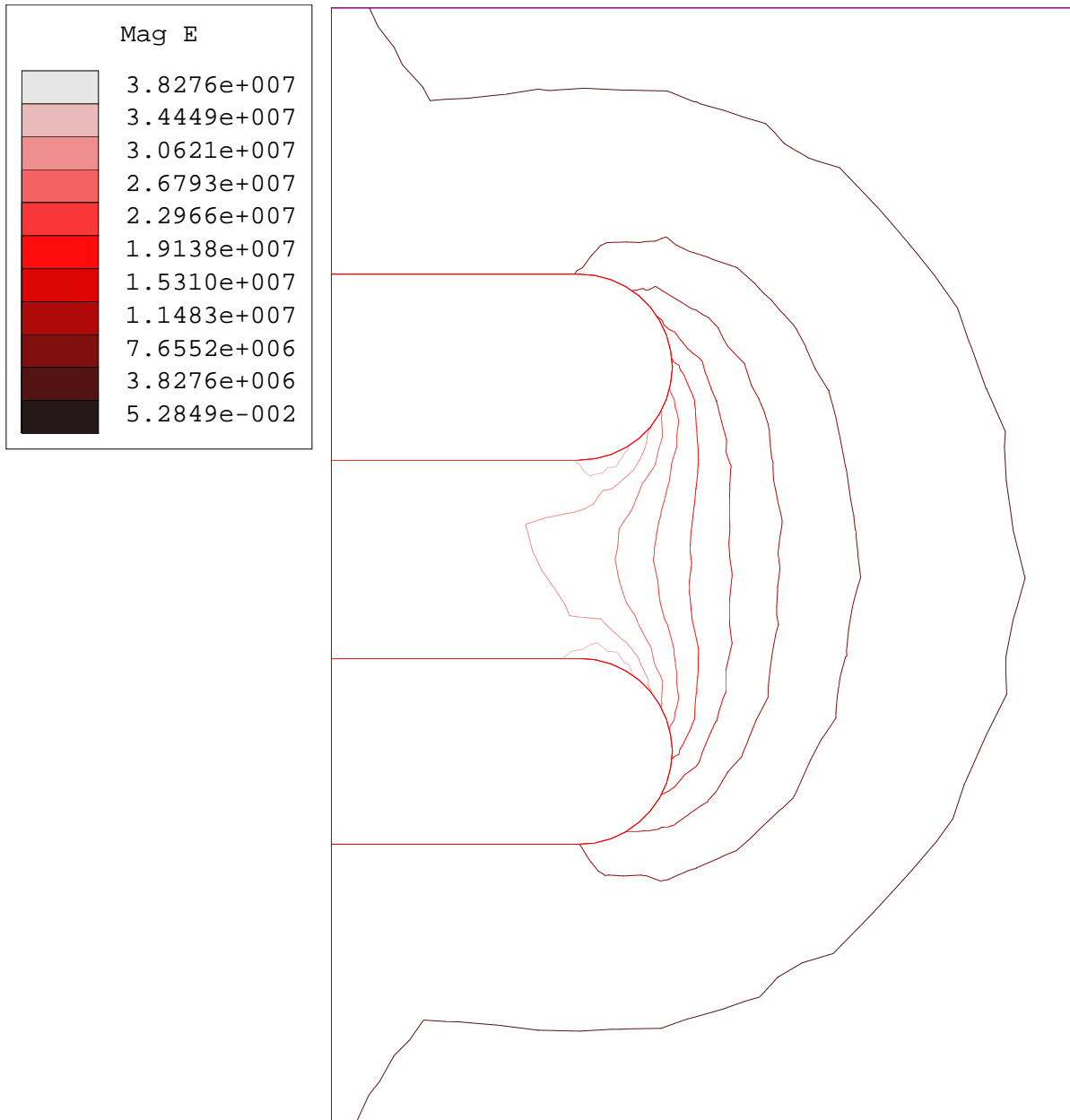3.8276e+006
5.2849e-002
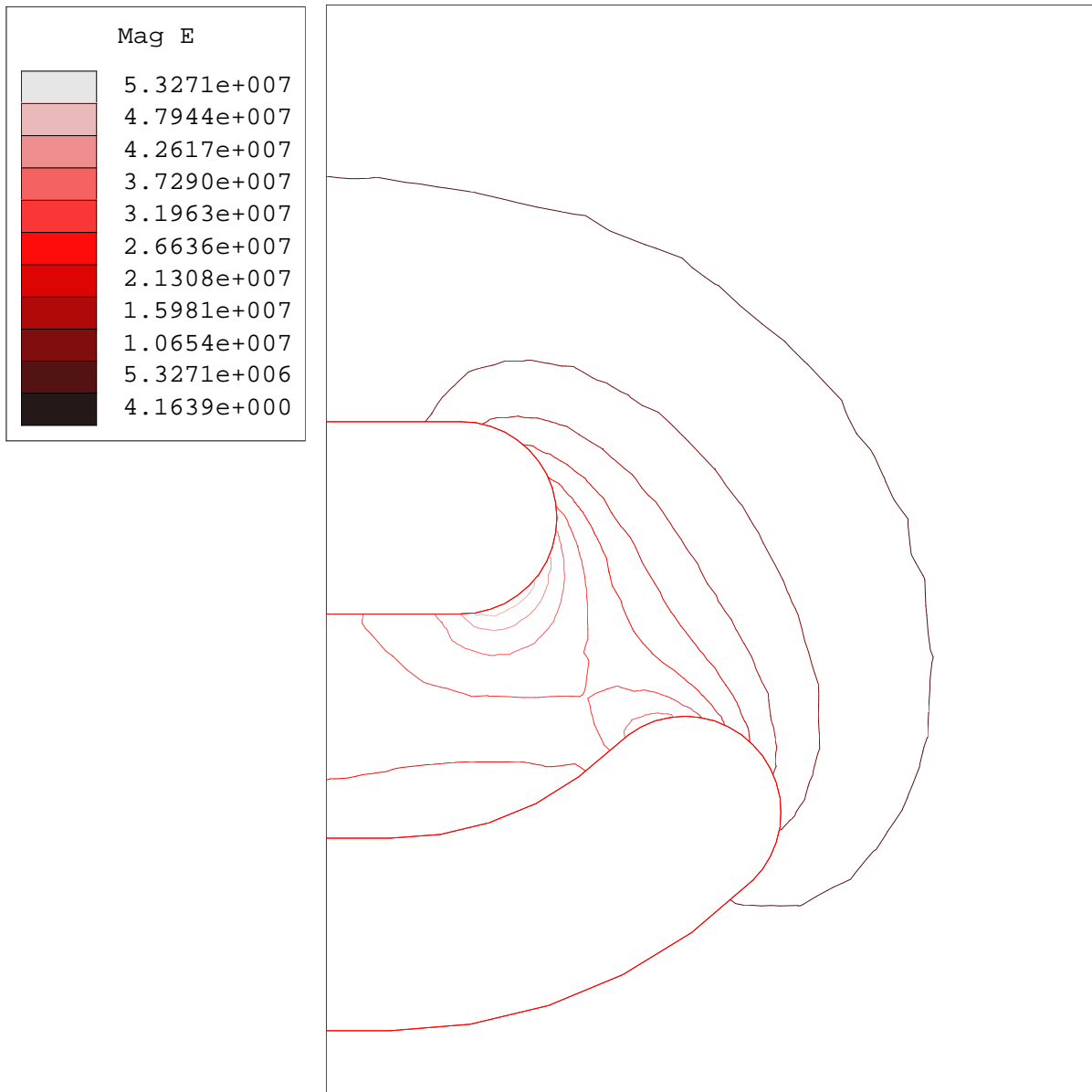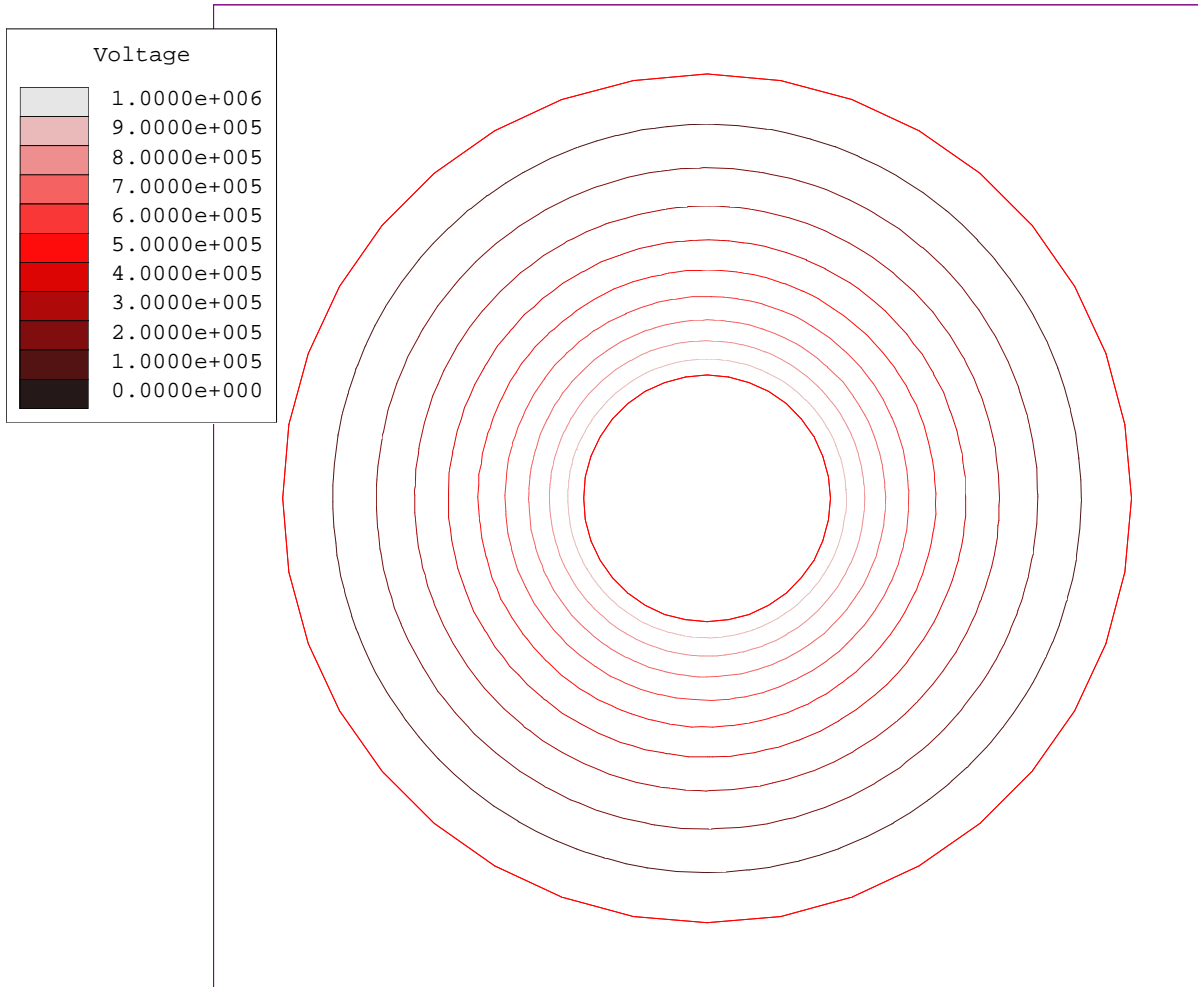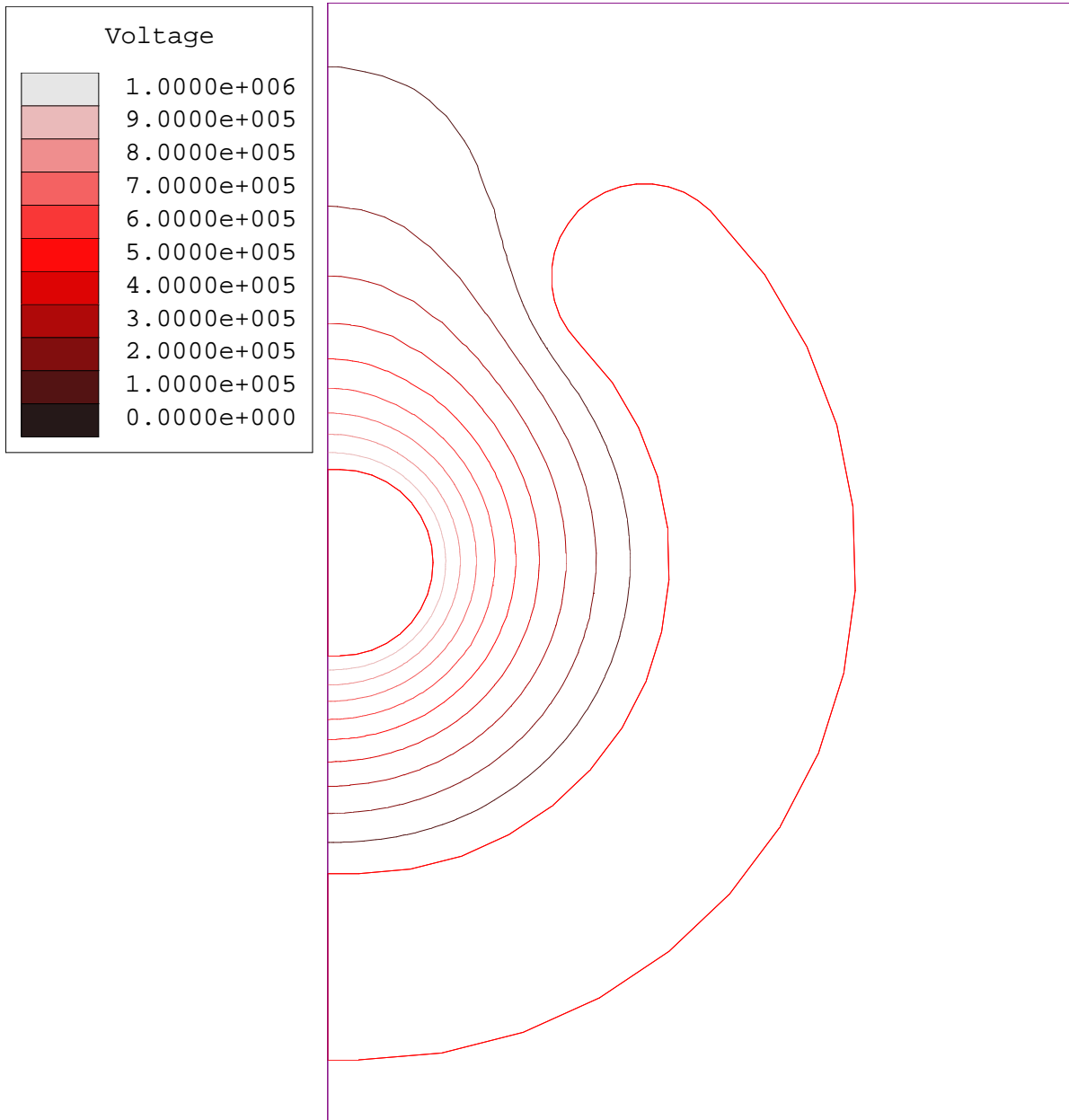
Figure 7.3. Voltages calculated by Maxwell. (Scale is in Volts.)

Figure 7.3. (con'd)

Figure 7.3. (con'd)

Figure 7.3. (con'd)

Voltage

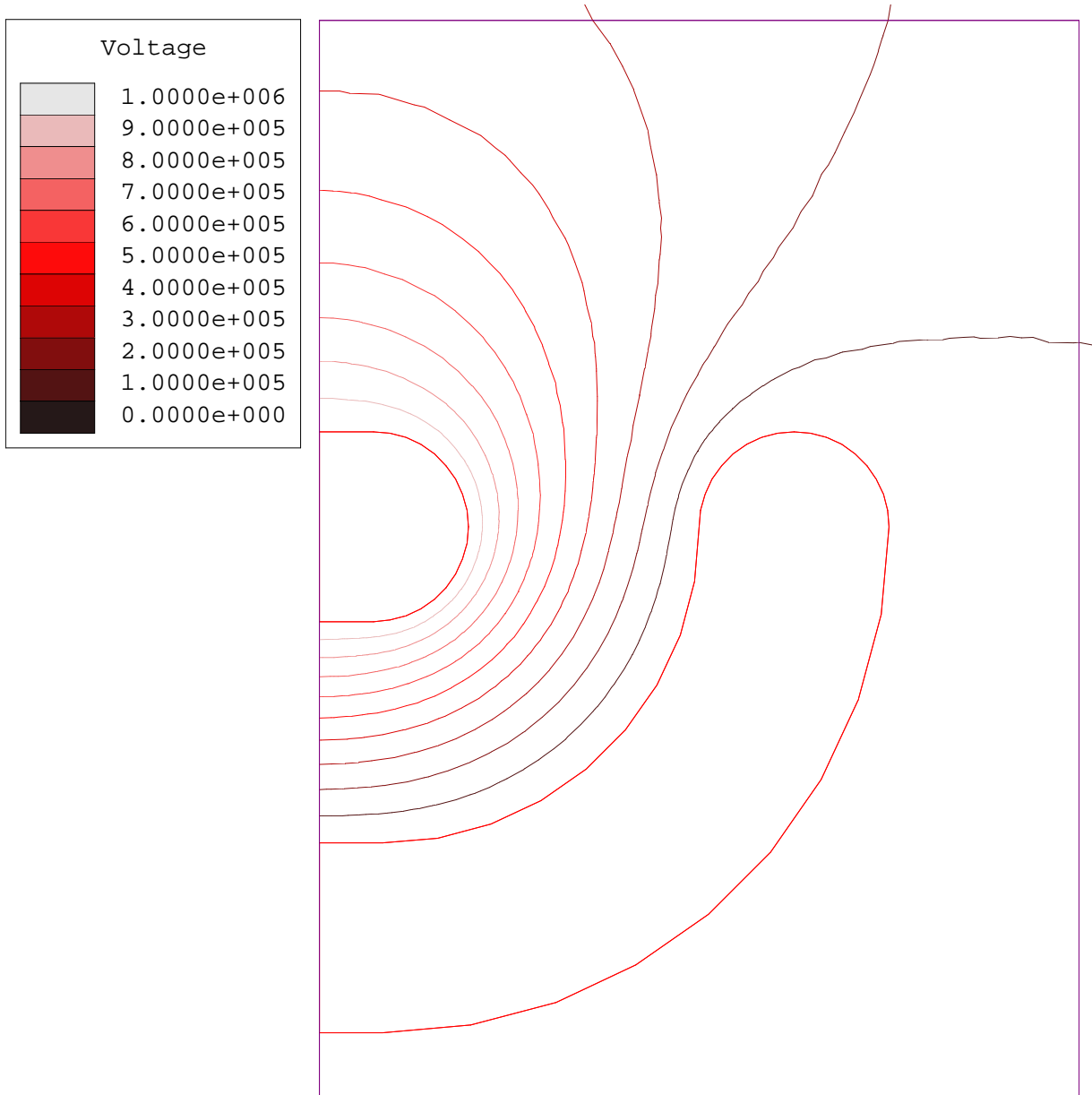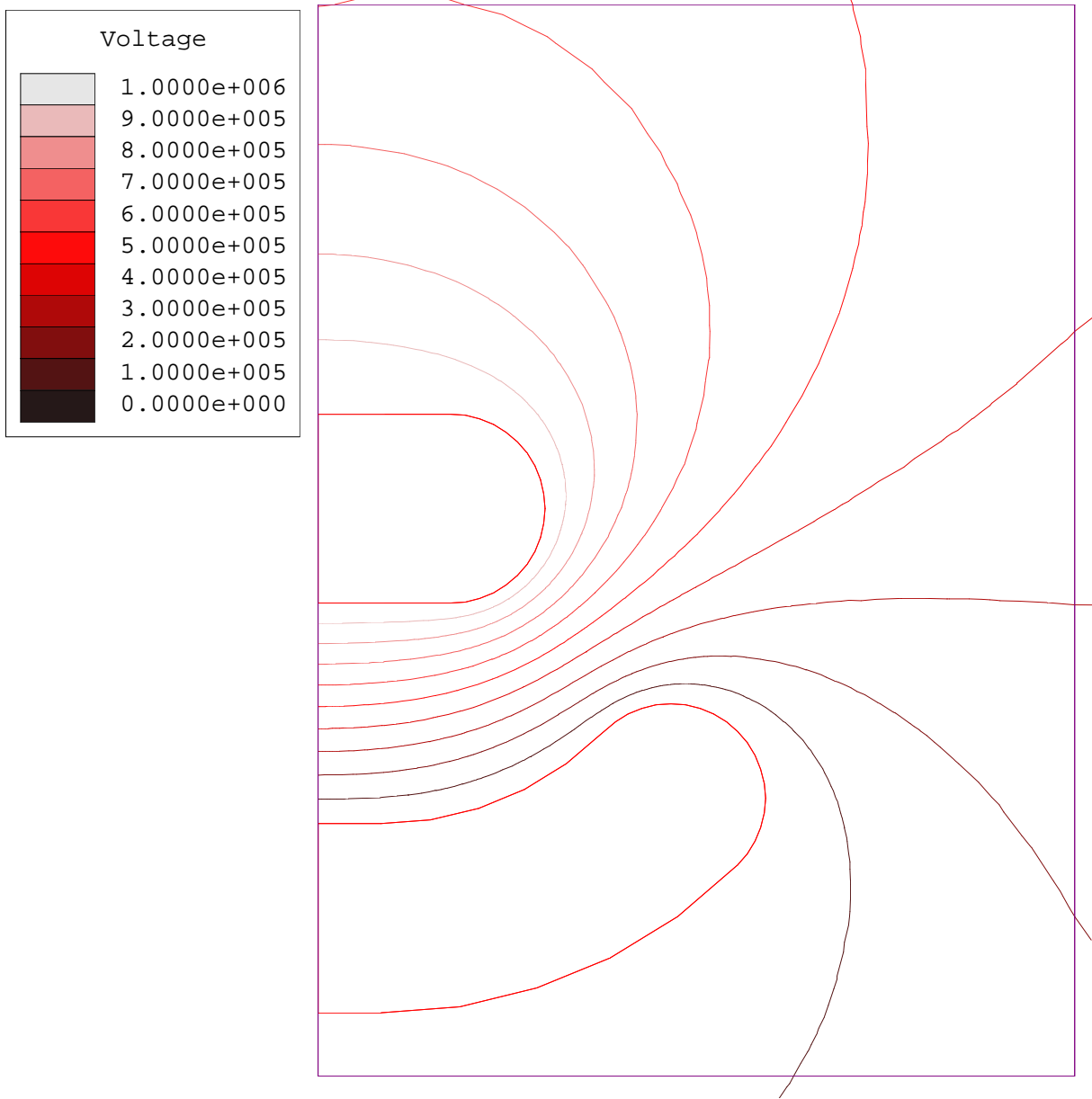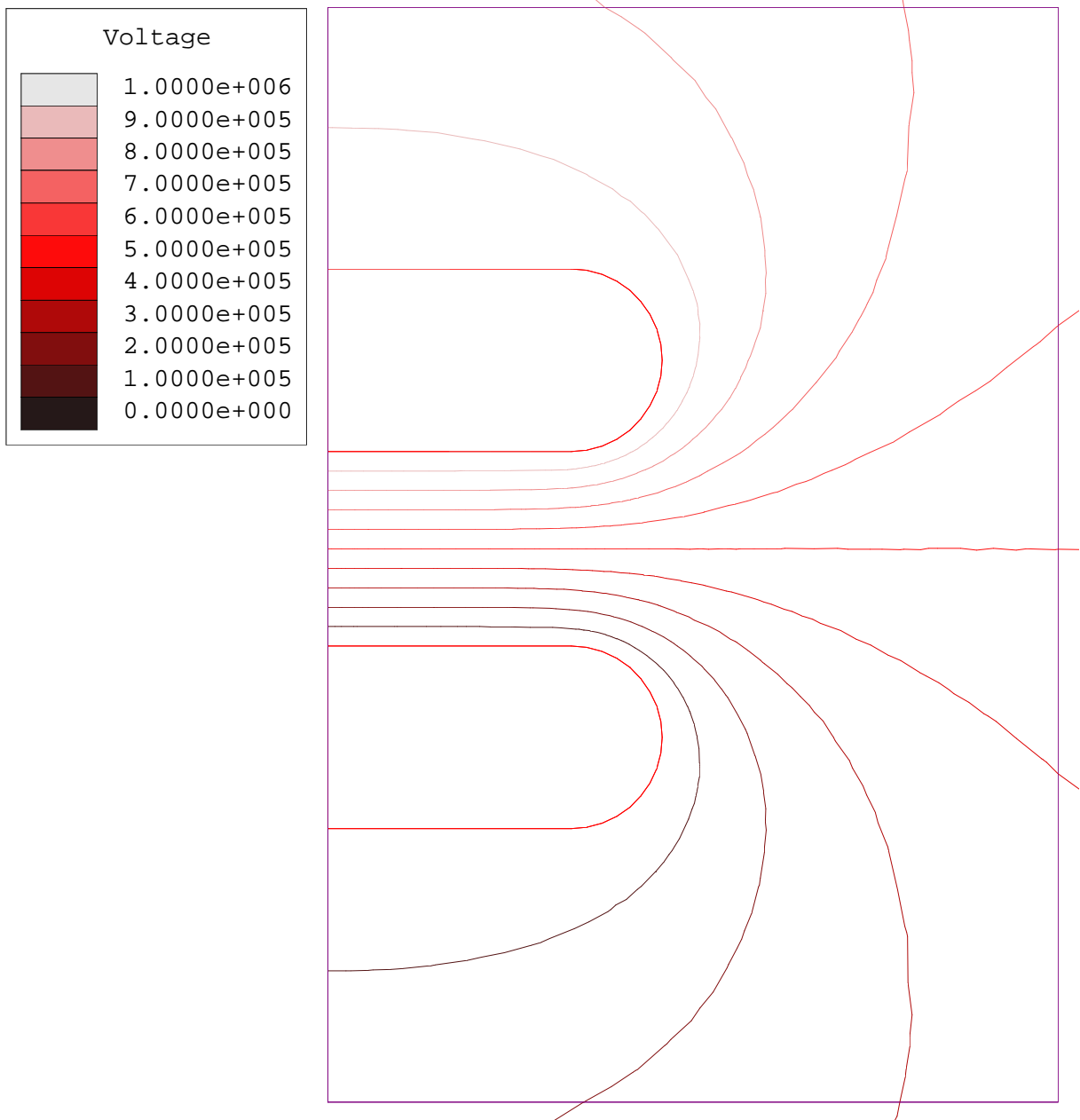|	
	1.0000e+006
	9.0000e+005
	8.0000e+005
	7.0000e+005
	6.0000e+005
	5.0000e+005
	4.0000e+005
	3.0000e+005
	2.0000e+005
	1.0000e+005
	0.0000e+000

Figure 7.3. (con'd)

VIII. The Effect of a Tapered Transmission-Line

A characteristic of any balun design will be a taper in the transmission line characteristic impedance. The output impedance of high-voltage sources is often around 5 Ω, whereas a typical antenna has an impedance of 100-400 Ω.

In the high-frequency (early-time) limit, the peak voltage scales as $Z_c^{1/2}$, where Z_c is the local characteristic impedance of the line. This has the effect of maintaining a constant peak power. Thus, for example, a 1 MV signal at 10 Ω becomes a 4.5 MV signal at 200 Ω. This additional voltage must be considered in the design.

In the low-frequency (late-time) limit, one has very different behavior. One can then think in terms of a circuit solution instead of a wave solution to the problem. Thus, one will need some resistors to damp out the low-frequency reflections from the end of the balun and antenna, or the device will look like an open circuit. However, note that in many circumstances it is just the early-time behavior that is of concern.

If one were interested in providing a more accurate model of the effect of the tapered transmission line, which would include the effects at intermediate frequencies, one would consider one of two methods. First, one could use a one-dimensional finite-difference time domain analysis to model the transmission through a line of varying impedance. Alternatively, for exponentially tapered transmission lines, one could use a closed-form analysis such as that provided by N. Younan et al in [9].

IX. Conclusions

We have summarized here much of the design criterion that is necessary to design coaxial unzipper type baluns for high powers and fast risetimes. We have shown why it is advantageous to perform the unzipping at low impedances. We have provided dielectric strength data for most of the common insulators one might use. A rule was derived for predicting the risetime of this class of baluns. Finally, a two-dimensional finite element analysis was performed at various points along the cross section, in order to calculate the impedance and the peak electric field.

Ultimately, the goal of a balun is to provide a suitable feed for an antenna. One approach for developing a suitable antenna for output of an unzipper-type balun is to us a lens Impulse Radiating Antenna (IRA). Some details on a possible design are provided in [13]

References

[1] C. E. Baum, Multi-conductor-Transmission-Line Model of Balun and Inverter, Measurement Note 42, March 93.

[2] C. E. Baum, Radiation of Impulse-Like Transient Fields, Sensor and Simulation Note 321, November 1989.

[3] C. E. Baum, Configurations of TEM Feed for an IRA, Sensor and Simulation Note 327, April 1991.

[4] E. G. Farr and C. E. Baum, Considerations for Ferrite Loading of a Balun, to appear shortly as a Measurement Note.

[5] L. Rinehart, personal communication.

[6] I. Smith, personal communication.

[7] R. J. Adler, *Pulse Power Formulary*, North Star Research Corp. August 1989.

[8] T. H. Martin, An Empirical Formula for Gas Switch Breakdown Delay, Proc. of the Seventh IEEE Symposium on Pulsed Power, pp. 73-79, 1989.

[9] N. H. Younan, B. L. Cox, C. D. Taylor, and W. D. Prather, "An exponentially tapered transmission line antenna," *IEEE Trans. Electromag. Compat.* Vol 35, No. 2, May 1994, pp. 141-144, and Sensor and Simulation Note 369.

[10] T. H. Martin, personal communication.

[11] C. E. Baum, The Conical Transmission Line as a Wave Launcher and Terminator for a Cylindrical Transmission Line, Sensor and Simulation Note 31, January 1967.

[12] Rex Schlicher, personal communication.

[13] E. G. Farr, Off-Boresight Field of a Lens IRA, Sensor and Simulation Note 370, October 1994.